Electron Spin Resonance (ESR)

Lendel Deguia, Nuno Mendes, Bryant Nguyen
Department of Physics, University of Texas at Dallas, Richardson, Texas 75080, USA

1. INTRODUCTION

Spectroscopy is the study of electromagnetic radiation interacting with matter — its origins can be traced back to Issac Newton and his sunlight dispersion experiment.[1] Spectrometry refers to the application of spectroscopic principles for experiments. Different forms of spectrometry exist which can be classified based on the nature of the interaction between the electromagnetic radiation and sample of matter involved in the experiment; types of spectroscopy include emission, absorption, or scattered-based spectroscopy. Our spectroscopy experiment focuses on a phenomenon known as electron spin resonance.

From quantum mechanics, it is known that electrons possess intrinsic angular momentum known as spin that can only exist in one of two states: spin up $m_s = 1/2$ or spin down $m_s = -1/2$ (*where m_s is the quantum magnetic number — each one correspondent to one of two possible values for the electron's intrinsic magnetic moment*). These spin states are degenerate for a free electron subjected to no interactions. However, an unpaired free electron in an atom subjected to some static magnetic field of magnitude B_0 will have its magnetic moment orient itself either parallel or anti-parallel to the field depending on its spin state where both orientations are associated with an energy given by $E = m_s g \mu_B B_0,\ m_s \in \{-\frac{1}{2}, \frac{1}{2}\}$. The expression for E clearly indicates that in the presence of a magnetic field, the spin states are no longer degenerate; the difference between the two energies is given by

$$\triangle E = g\mu_B B_0. \tag{1}$$

Here, g is the g-factor and μ_B is the Bohr Magneton. The g-factor is a dimensionless quantity which characterizes another quantity known as the gyromagnetic ratio γ (which characterizes the relationship between the electron's spin and magnetic moment) given by

$$\gamma = g\mu_B/\hbar$$

where $\hbar$ is a form of Planck's constant.

If in addition to the static magnetic field, the electron is also subjected to electromagnetic radiation of a particular frequency ν, depending on the spin state, the electron will either absorb or emit a photon of energy $E = h\nu$ ($h = 2\pi\hbar$) and transition into the other spin state such that the transition satisfies the resonant condition:

$$h\nu = g\mu_B B_0. \tag{2}$$

The relationship given by equation (2) is fundamental to ESR spectroscopy. For some sample possessing unpaired electrons subjected to a magnetic field with strength B_0 and irradiated with electromagnetic radiation of the resonant frequency ν, assuming we have an appropriate experimental set-up, the spin state transitions will yield a signal that can be detected. Analysis of this signal can provide insight into various properties of the sample material.

In proceeding sections, an experiment will be described to characterize the phenomena of ESR. Objectives of the experiment, along with an experimental setup will be described. Results will be described, and related to the fundamental formulas of interest, and inferences about ESR methodology will be developed to ascertain this method's viability for characterization.

2. METHOD

2.1. Objectives

Theoretically, we can study the relationship given by (2) by isolating an electron, subjecting it to a static magnetic field, and observing its behavior under the influence of electromagnetic radiation within some range of frequencies. However, in the presence of a static magnetic field alone, the electron will undergo uniform circular motion, and further addition of a sinusoidal electromagnetic field at resonance will provide a helical component to its motion; the resonant frequency serves as a resonant driving frequency towards the electron's motion, and in this case, it will be difficult to acquire information about its quantum spin state since the resonant electromagnetic energy corresponds to its orbital angular momentum (not its spin angular momentum). Furthermore, if multiple electrons were to be considered, there would be the additional complication of the electrons repelling each other.

Our goal with ESR is to acquire information about the material the electron makes a spin transition within; of course, the aforementioned electron would not give us any information about any material even if we could somehow get it to possess only spin angular momentum (that is, to "spin" in place) since, well, it's a free electron. Therefore, for an ESR experiment, we want the electron to be inside some material and we want the electron to have zero angular momentum. We also want to minimize the interaction of an electron with its environment such as with other electrons and neighboring nuclei.

This experiment focuses on two crystal forms of organic compounds that closely satisfy these conditions: Tetracyanoquinodimethane (TCNQ) and 2,2-Diphenyl-

1-Picrylhydrazyl (DPPH). DPPH is a free radical that has a molecular structure such that one of its nitrogen atoms has a free electron. TCNQ is an organic anion that has a high electron affinity (i.e. it is a strong electron acceptor) such that when paired with an appropriate organic cation (the electron donor), forms an ion-radical salt which serves as a free radical compound like $DPPH^2$.

The objective of this experiment is to acquire a resonance signal from these compounds and investigate the properties of that signal. After processing, the signal should manifest as a spectral line. However, in reality, the electrons are subjected to interactions with their surroundings, so instead, we will end up with a spectral curve. The g-factor along with the relaxation times of the sample and the linewidth of the corresponding spectral curve are quantities that warrant our primary attention. For a free electron, the g-factor is (up to ten significant figures) $g_e = 2.002319304$. Any departure from a spectral line and the electron g-factor is indicative of the electrons inside the material being influenced by external interactions; it is these departures that are able to provide information about the properties of the material the electrons are inside.

2.2. Detection and Experimental Set-Up

The apparatus used for the experiment is depicted in figure 1. Equation (2) indicates a linear relationship between the electromagnetic signal frequency and the static magnetic field which provides two implicit approaches to an ESR experiment: we can hold the static magnetic field strength constant and sweep through different frequency values or we can hold the frequency constant and sweep through different magnitudes of the static magnetic field. We use the latter approach because the apparatus we use provides a smoother signal this way. Since the resonance signal will have a spread and since the experiment operates at a single frequency, each swept value of the magnetic field will correspond to an emitted signal at the set frequency at different amplitudes such that the amplitude of the emitted signal is maximum precisely at resonance.

Detection of the ESR resonance signal relies primarily on the interaction between the sample material and an amplifying resonant circuit (called an Autodyne circuit). The resonant circuit is what provides the electromagnetic signal (microwaves) to the sample via an alternating current/voltage at the set frequency ν. The sample is placed into a probehead which is positioned such that the sample is inside a solenoid connected to the resonant circuit and hence, subjected to the alternating magnetic field inside the solenoid. Simultaneously, the sample is positioned between the two halves of a Helmholtz coil which provides the static magnetic field.

At resonance, there will be a transition in free electron spin states which will cause energy dissipation at the solenoid (we assume the paramagnetic species is in thermodynamic equilibrium so according to the Maxwell-Boltzmann distribution, the majority of electrons will be in the spin down state and thus, will absorb energy to make their transitions). This energy dissipation at the solenoid will cause a reduction in the quality factor of the circuit (where the quality or Q factor is proportional to the ratio of the energy stored to the energy dissipated in the circuit). It is precisely this reduction of the Q factor that provides our resonance signal.

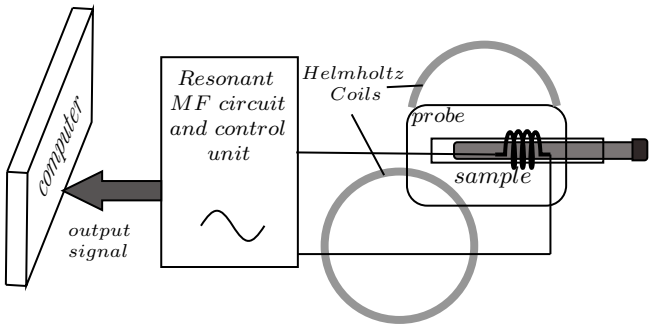

FIG. 1: Simplified Diagram of our ESR Apparatus

However, the signal provided by this reduction is very small which our apparatus can not adequately amplify. Instead, our apparatus contains a modulation component which modulates the static field to sinusoidally fluctuate (at about 38 Hz) within a small neighborhood of the static field strength, so for each swept value of the magnetic field, we end up with two different emitted intensities. We still end up with a signal at frequency ν, but this signal alone will obscure the applied modulation. Instead, the emitted signal is ran through a filter such that the output of the filter provides a signal at the modulation frequency that fluctuates between the two emitted intensity values. Consequently, this ends up providing us with a differential output which, after the field sweep, manifests as the derivative of the resonance curve; we then can use numerical integration to extract the resonance curve. This process is illustrated in figure 2.

Although we are not performing a frequency sweep, we perform the experiment at different frequency values (within a small neighborhood of 50 MHz) in order to acquire different resonance points. We will then map out these points via the relationship given by (2) so that the points hopefully end up forming a linear plot. From there we can evaluate the slope of the plot and hence, the g-factor. Our apparatus is connected to a computer where a program provided with the apparatus evaluates the g-factor for the user, so we will also compare the line fitted g-factor value with the arithmetic mean of the ones provided by the software.

It is predicted that the collective magnetization of the electrons in the samples will provide a spectral curve which will be given by

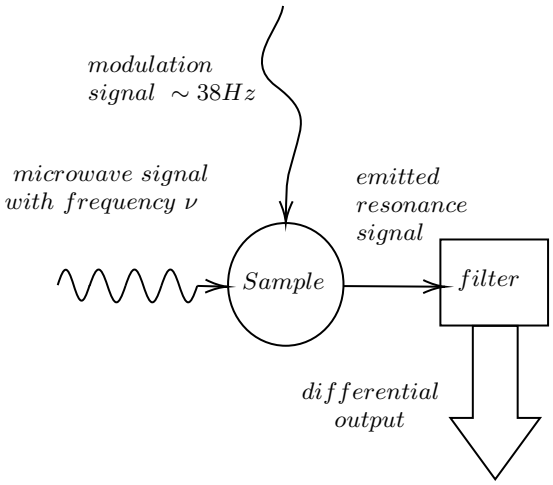

FIG. 2: Modulation Process

$$F(H) = \frac{\gamma T_2}{\pi} \frac{1}{1 + \gamma^2 {T_2}^2 (H - H_0)^2} \tag{3}$$

where H is the auxiliary magnetic field value (which is effectively what our apparatus detects due to various material properties present throughout the set-up) and T_2 is the transverse relaxation time. After collecting data, we also want to compare our derived resonance curves to the one given by (3). The transverse relaxation time is related to the amount of time it takes for the transverse components of the overall magnetization of the sample to decay from the net dephasing of the electron spin ensemble after being perturbed by the microwave signal, and it is related to full width at half-maximum of the curve $\triangle H$ (FWHM; i.e. the line width) by[2]

$$T_2 = \frac{\sqrt{2}}{\gamma \triangle H} \tag{4}$$

3. RESULTS AND ANALYSIS

We compile results in terms of the derivative ESR curves, and their integrals (the absorption curves) for both materials. These are shown in figure 3, in which the signal amplitude vs. magnetic field are shown for a pair of representative frequencies (namely, 49MHz, and 50.5MHz). One can make a few inferences between frequencies that are held for both materials.

Both in the derivative, and integrated ESR curves, a horizontal shift rightwards can be seen for increasing frequencies. This can be explained fully by the change in frequency, that directly leads to a change in B_0. Clearly, from (2):

$$\nu = \frac{g \mu_B B_0}{h} \tag{5}$$

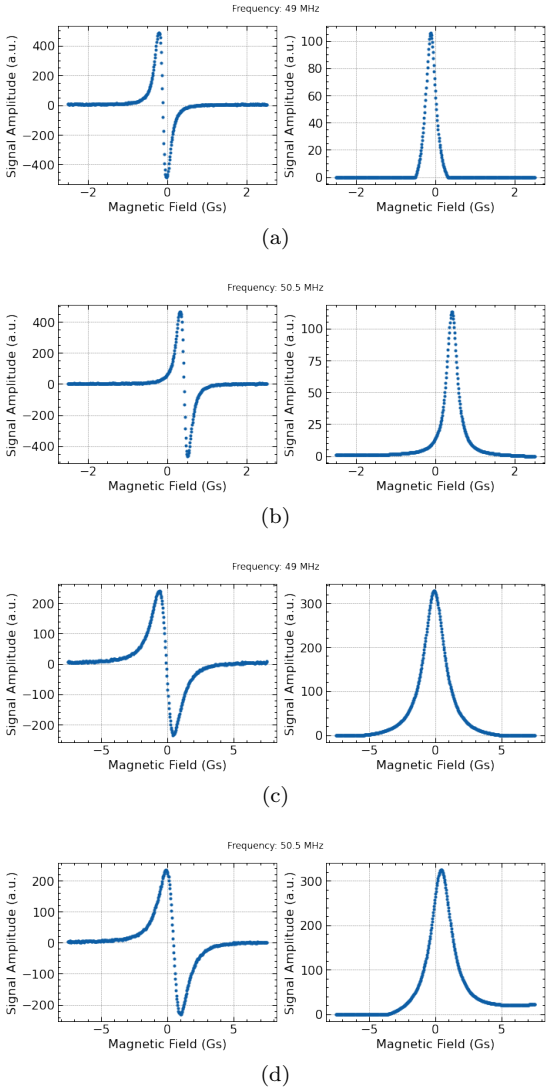

FIG. 3: Graphs of signal amplitude (a.u.) vs. magnetic field (Gs) for TCNQ (3a. with 49 MHZ, and 3b. with 50.5 MHZ), and DPPH (3c. with 49 MHZ, and 3d. with 50.5 MHZ). Left graphs depict derivative ESR curves, with graphs on the right depicting the integral of each derivative curve. Both sets of graphs show a significant shift rightwards in the graph when increasing frequency.

The zero-crossing in the derivative curves, and the peak signal amplitude in the absorption curves correspond to magnetic fields within the critical value (the very middle) of the bandwidth of resonant frequencies.

Figure 4, however, depicts a graph of the frequency plotted against the static magnetic field applied. From equation (2), we can derive an expression for g:

$$g = \frac{h\nu}{\mu_B B_0} = \nu / (\frac{B_0 \mu_B}{h}) \tag{6}$$

Thus, the slope of the frequency vs. $\frac{B_0 \mu_B}{h}$ over a multitude of points represents an accurate estimate of the g-values for our samples. Through fig 4: $\mathbf{g_{TCNQ}} = 1.960$,

and $\mathbf{g_{DPPH}} = 1.957$. These represent apt estimates, and close approximations to real values for g in TCNQ[3,4].

We also evaluated the mean FWHM and relaxation time for TCNQ to be $\triangle H = 0.31\ Gs$ and $T_2 = 2.65 \times 10^{-7}\ s$ respectively and for DPPH to be $\triangle H = 1.80\ Gs$ and $T_2 = 4.56 \times 10^{-8}\ s$ respectively (where $\triangle H$ was used along with the g-factor in equation 4 to evaluate T_2). When taking into account these parameters for equations (3) and (4) while taking into account the gain delegated onto the samples by the apparatus, we find there is a slight deviation between the Lorentzian curve provided by equation (3) and the ones evaluated from our derivative data through numerical integration. This deviation is most likely explained by the fact that equation (3) is based on macroscopic assumptions and does not take into account every single electron magnetic moment present throughout the samples (it uses net magnetization instead). Nevertheless, the deviations are not too significant despite these assumptions. For instance, to compare the Lorentzian in eq. 3 to our integral curves, figure 5 depicts the curve evaluated using equation (3) for TCNQ at 49MHz. Clearly, we can find similar functional behavior from our integral curves in figure 5.

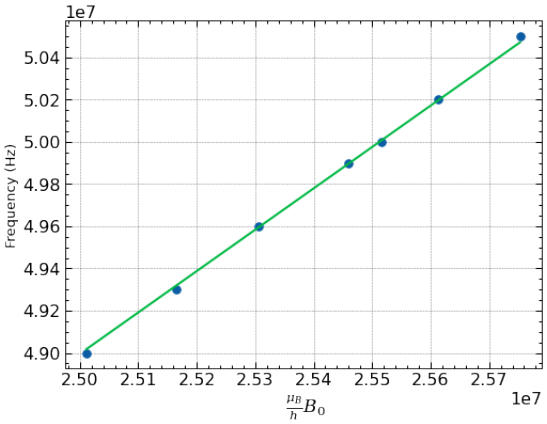

(a)

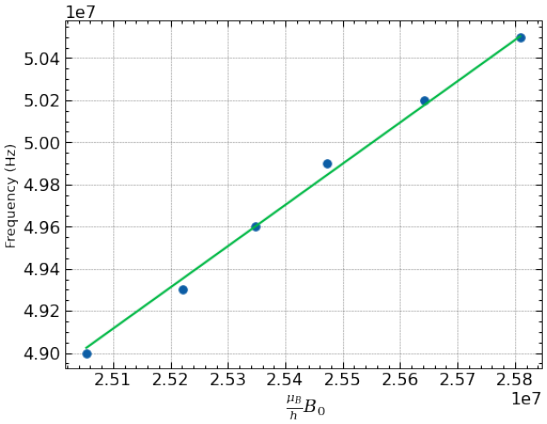

(b)

FIG. 4: Frequency vs. "normalized" static magnetic field. Best-fit line provides for the g-factor in each material. $g_{TCNQ} = 1.960$, and $g_{DPPH} = 1.957$.

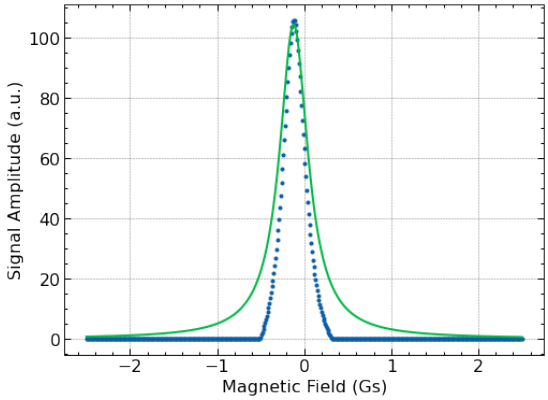

FIG. 5: Integral graph in fig 3 for 49MHz TCNQ in blue, and theoretical curve using equation (3) in green.

4. CONCLUSIONS

Our g factors differed from the indicated electron g factor as indicated by the following

$$\frac{|g_e - g_{TCNQ}|}{g_e} \times 100 = 2.12\%$$

$$\frac{|g_e - g_{DPPH}|}{g_e} \times 100 = 2.27\%$$

Moreever, using the data collected from the experiment, we calculated g factors of TCNQ and DPPH that are extremely similar to the ones calculated by the software. As stated before, the difference between our values and the software's is most likely explained due to a discrepancy in the significant figures of each variable. Moreover, our findings for the value of g_{TCNQ} are corroborated by a study performed in 2006 that used a quantum electrodynamics calculation[4]. However, a study performed by Voesch et al. found multiple values of g_{DPPH} near 0K that are higher than the ones that we calculated. Their data shows a negative relationship between g_{DPPH} and temperature[5], but we believe more experimentation is needed to properly understand the difference between our findings. If we were to perform this experiment again, we would heavily consider running the samples at a wide range of temperatures. Also, as mentioned before, the increase of B_0 with frequency is as we expected from analysis of equation 2.

As indicated earlier, the discrepancy between our g factor values and the one for the electron is likely due to interactions the electrons in each sample are subjected to such as with neighboring nuclei and other electrons; these

interactions affect the net magnetization detected which then corresponds to affecting the g factor and FWHM evaluations. Another possible source of error in our experiment can be attributed to too few firxed frequencies being run. We only ran 6 and 7 different frequencies for DPPH and TCNQ, respectively. If we had run the experiment at more different frequencies (say in increments of 0.1MHz or 0.05MHz instead of 0.3MHz), it is possible that we would have gotten more accurate results, and in turn, more accurate calculations of the g factors. Another source of error could be the settings for the gain while performing the experiment. We found that for different gain settings, the software would output different values for g and $\triangle H$. It is possible that the difference in those values could stem from noise from the sensor and that a higher gain could help to minimize its effect.

5. AUTHOR CONTRIBUTIONS

All authors contributed to collection of data. L. Deguia wrote and generated the diagrams for the introduction and the method sections, compiled the data into csv files, and processed/organized them in python ready to be polished and extracted. N. Mendes wrote the section "Results and Analysis" for the report, extracted the data from the python file, contributed to design of the plots, and made the bibliography. B. Nguyen wrote the conclusion, and chose some references of interest, in addition to reviewing the report.

[1] A. Frankoi, D. Morrison, and S.C. Wolff. 5.3 spectroscopy in astronomy - astronomy, Oct 2016.

[2] M. T. Jones. Spin—Lattice Relaxation in Some TCNQ Ion—Radical Salts. *J. Chem. Phys.* , 40(7):1837–1842, April 1964.

[3] Y. Tomkiewicz, A. R. Taranko, and J. B. Torrance. *g*-value decomposition of magnetic susceptibility in tetrathiafulvalene- and hexamethylenetetrathiafulvalene-tetracyanoquinodimethane (ttf-tcnq and hmttf-tcnq). *Phys. Rev. B*, 22:3113–3118, 1980.

[4] B. Odom, D. Hanneke, B. D'Urso, and G. Gabrielse. New measurement of the electron magnetic moment using a one-electron quantum cyclotron. *Physical Review Letters*, 97:3, July 2006.

[5] W. Voesch, M. Thiemann, D. Bothner, M. Dressel, and M. Scheffler. On-chip esr measurements of dpph at mk temperatures. *Physics Procedia*, 75:503–510, 2015. 20th International Conference on Magnetism, ICM 2015.